Lecture 12 – SPECT

This lecture will cover: *(CH3.11-3.12)*

- Single Photon Emission Computed Tomography (SPECT, 单光子发射CT)
  - Instrumentations
  - Data processing in SPECT
    - Scatter correction
    - Attenuation correction
    - Image reconstruction
  - SPECT/CT
- Clinical application of Gamma camera and SPECT

(*Supplementary reading: The Essential Physics of Medical Imaging CH19.1-19.2)*

Instrumentation

- 2-3 gamma camera rotate around the patient
- Detecting γ-rays at a number of different angles
- Filtered backprojection or iterative techniques used to reconstruct multiple 2D axial slices
- Same instruments and radiotracers used as planar scintigraphy (gamma camera)

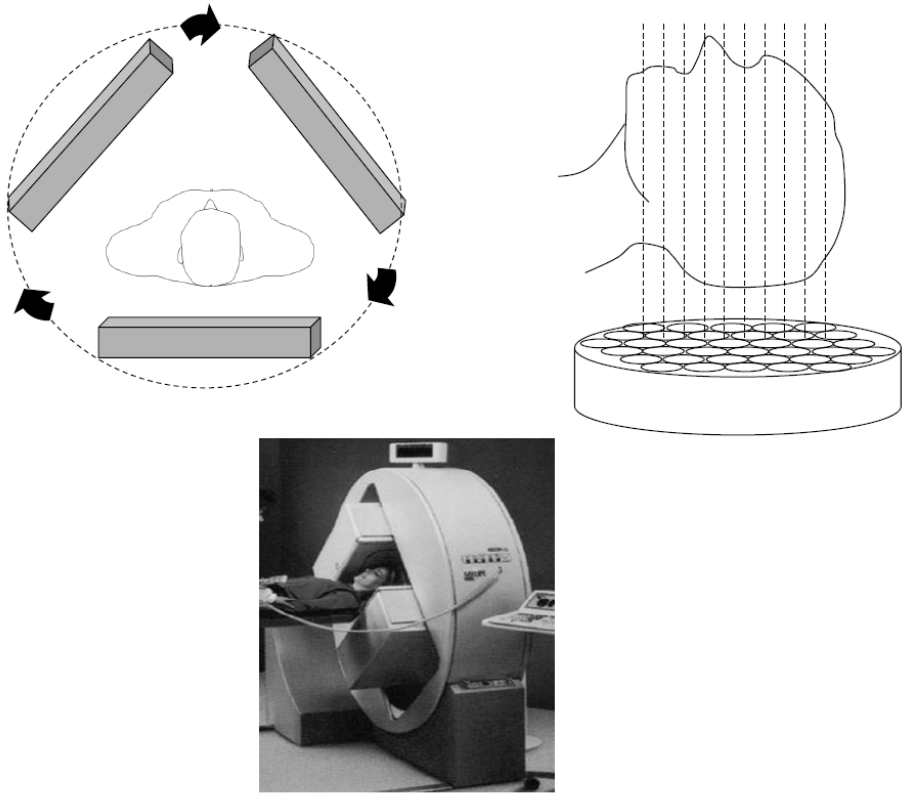

Fig. (top left) A three-head rotating gamma camera SPECT system for imaging the torso. (top right) Multiple 2D slices can be acquired in the longitudinal direction. (bottom) A 2-head SPECT camera: the heads can be moved inwards to image the brain, or outwards for the body.

Data acquisition

- A 360° rotation is generally needed since the projections acquired at 180° to one another are not identical. The source-to-detector distance affects
  - the distribution of γ-rays scatter in the body
  - the degree of tissue attenuation
  - The spatial resolution
- A converging collimator is often used to increase SNR;
- Slice thickness is determined by the position network of camera (spatial resolution of the camera);
- Typical 100000-500000 counts per image with a spatial resolution of 7mm above.

Scatter correction

- The accepted range of energies can result in the detection of scattered γ-rays with large angles up to 50^{o} ;
- The higher concentration of radiotracer, the greater number of scattered γ-rays;
- Position-dependent scatter correction is required
- Multiple energy windows based on the output of the multi-channel analyzer are used for the correction;

Steps of correction

- Primary and secondary projections are determined by using separate energy windows;
  - **Primary window:** centered at the photopeak and containing contribution from both scattered and unscattered γ-rays
  - **Secondary window:** locating beside primary windows and containing contribution only from scattered γ-rays
- The count of scattered γ-rays from secondary projection is subtracted from the primary projection by a scale factor calculated from the width of energy windows;
- The subtraction for projection is based on pixels

Correction windows

- **Dual-energy window approach**
  - A scale factor of $W_m/2W_s$,

  where

  W_m : the width of primary window (127-153keV for ^{m}Tc99)

  W_s : the width of secondary window (92-125keV for ^{m}Tc99)

  and 2 is determined empirically

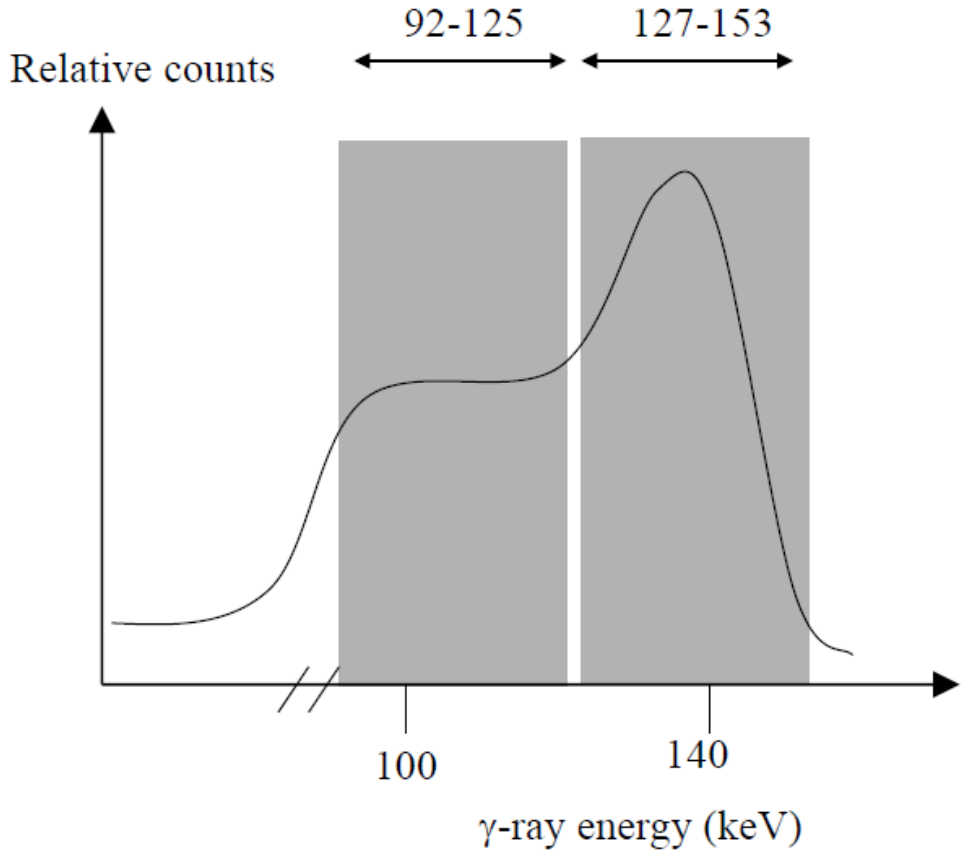

Fig. Scatter correction for SPECT: A dual-energy window approach.

Correction windows

- **A triple-energy window (TEW) approach:**
  - Primary window: 15% centered at photopeak (129.5-150.5keV)
  - Secondary window: 3kev centered at 126 and 153keV
  - Divide the count of scattered projection by the width in keV and add together for the two secondary window, and multiply the result by half of the primary window width, finally subtract the scatter counts from primary projection

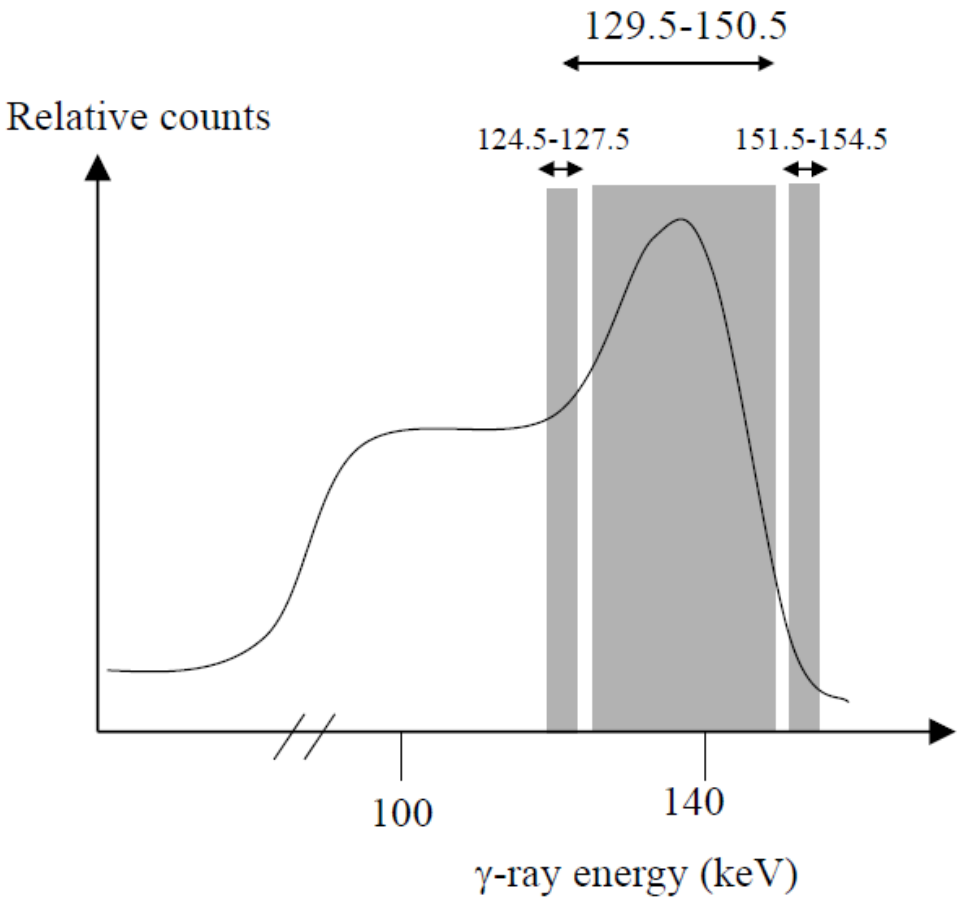

Fig. Scatter correction for SPECT: a triple-energy window approach.

Attenuation correction

- The γ-rays from deeper within the body are attenuated more;
- Correction method
  - **Chang's multiplicative method:**
    - ✓ Assume tissue attenuation coefficient uniform throughout the body being imaged
    - ✓ Steps of the correction:
      1. Find an initial image by filtered backprojection without any correction
      2. Use the initial image to determine the distances that γ-rays travel
      3. Scale up each projection by an appropriate factor given by $e^{\mu x}$
    - ✓ Reasonable for brain and abdomen scan, but not used for cardiac or thoracic imaging due to highly spatial dependent tissue attenuation
  - **Accurate attenuation coefficient correction:**

    Acquire a transmission scan using ^{153}Gd, calculate attenuation coefficient at each position and then correct the image from radiotracer.

Attenuation correction

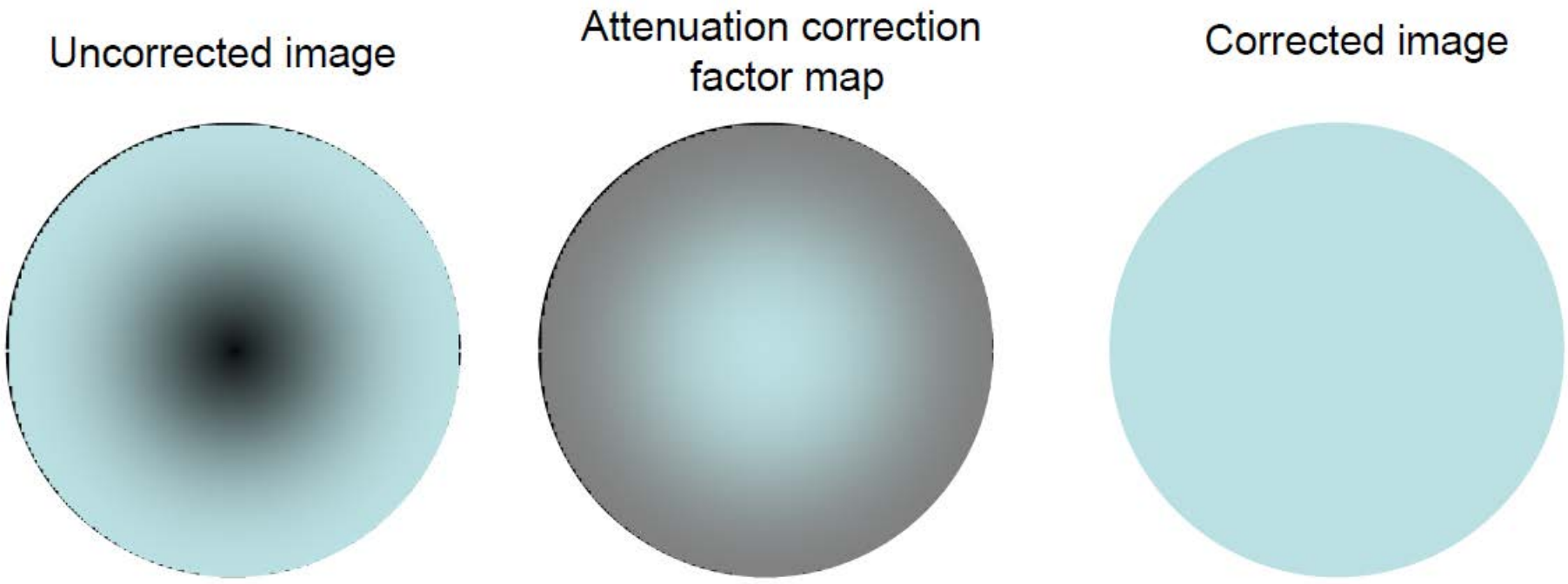

Fig. Demonstration of Chang's multiplicative method for attenuation correction. (left) An uncorrected SPECT image of a sphere which is filled with a material with uniform radioactivity. The dark area in the middle occurs since γ-rays are attenuated as they pass through the material. (middle) Based upon the outline of the phantom, a correction factor map is produced, with a high scaling factor at the centre and lower scaling factor to the outside. (right) Application of the correction factor gives an image which reflects much more accurately the uniform distribution of radiotracer.

Image reconstruction

- Filtered backprojection
- Iterative methods

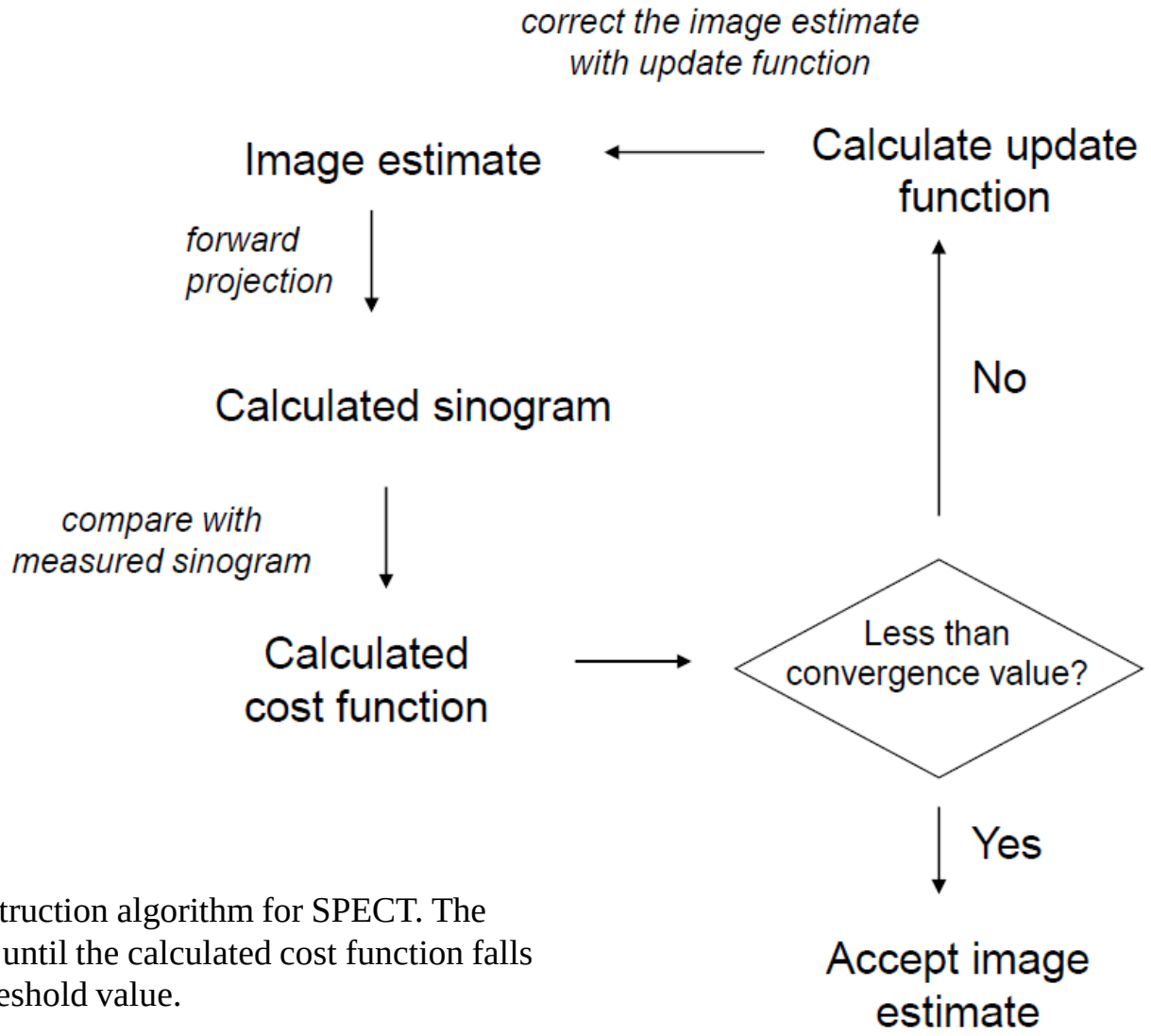

Fig. An iterative reconstruction algorithm for SPECT. The algorithm loops around until the calculated cost function falls below a pre-defined threshold value.

SPECT/CT

➢ **Combined scanner of SPECT and CT with advantages :**

- Improved attenuation correction of SPECT than isotope based transmission scan;
- The fusion of high-resolution anatomical (CT) and functional (SPECT) information with reduced partial volume effects compared to SPECT alone.

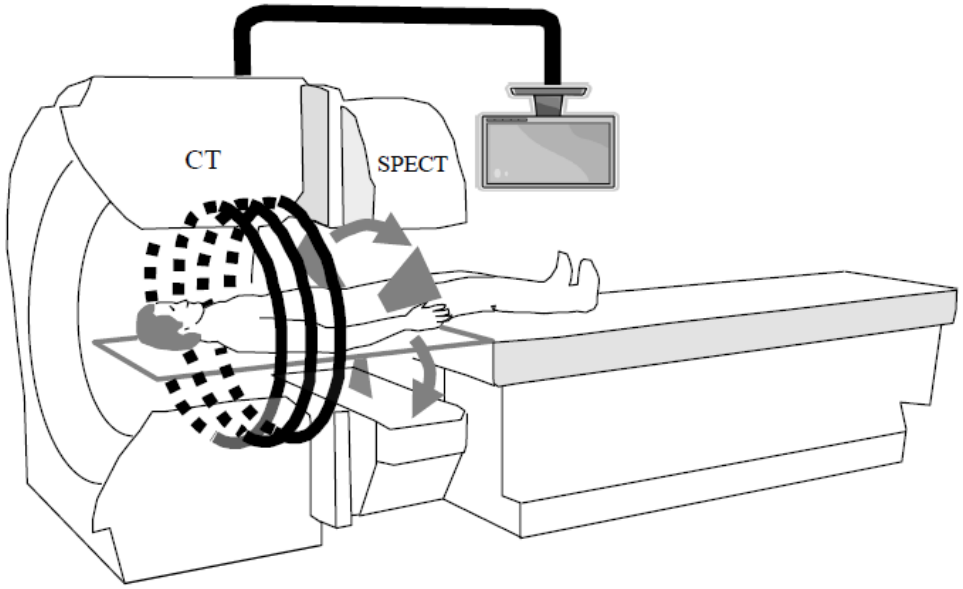

Fig. (left) A SPECT/CT system using a shared bed for the patient. (right) A commercial system. There are two gamma cameras, one above and one below the patient, and a circular entry for the multi-detector CT..

Lecture 12 – SPECT

This lecture will cover:

– Single Photon Emission Computed Tomography (SPECT, 单光子发射CT)

- Instrumentations
- Data processing in SPECT
  - Scatter correction
  - Attenuation correction
  - Image reconstruction
- SPECT/CT

– Clinical application of Gamma camera and SPECT

Bone metabolism

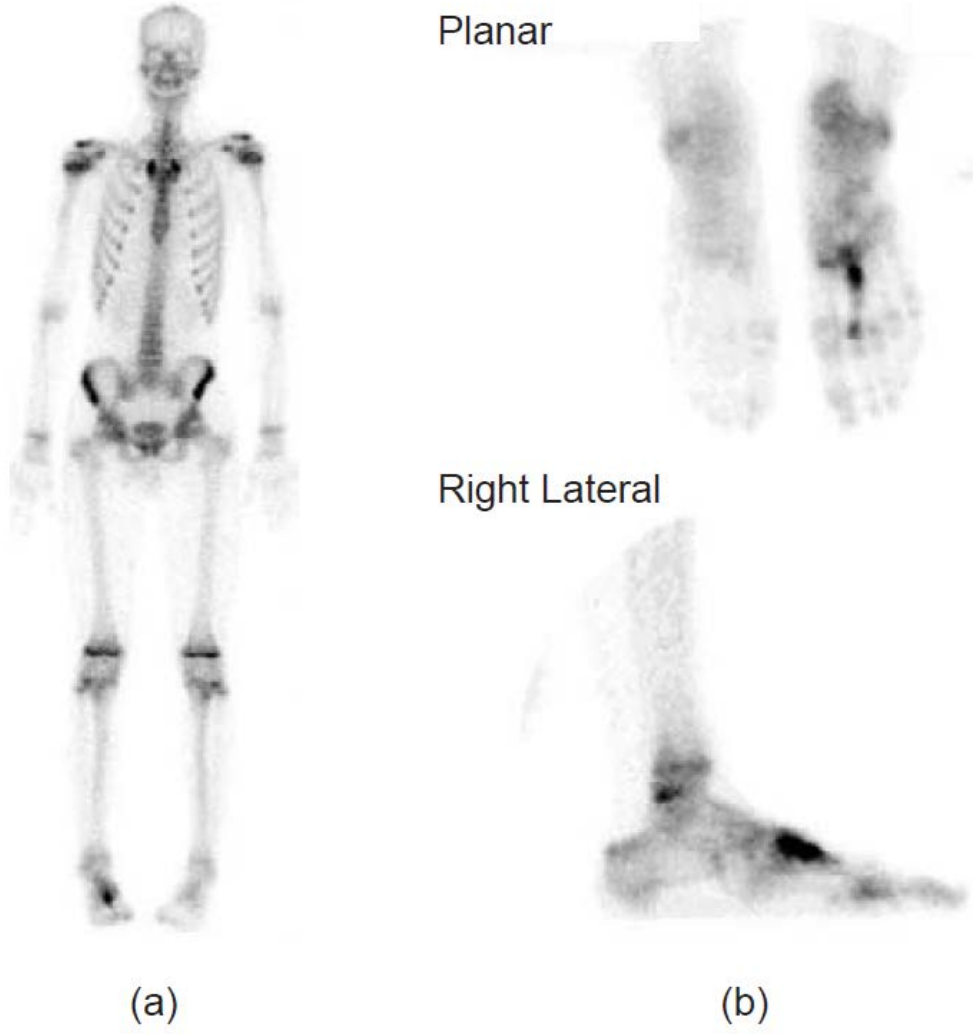

Fig. Left: whole-body scintigraphy after injection of 25 mCi ^{99m}Tc-labeled methylene diphosponate. This patient suffers from a stress fracture of the right foot. Right: control scans show an increased uptake in the metatarsal bone II compatible with a local stress fracture..

Myocardial perfusion

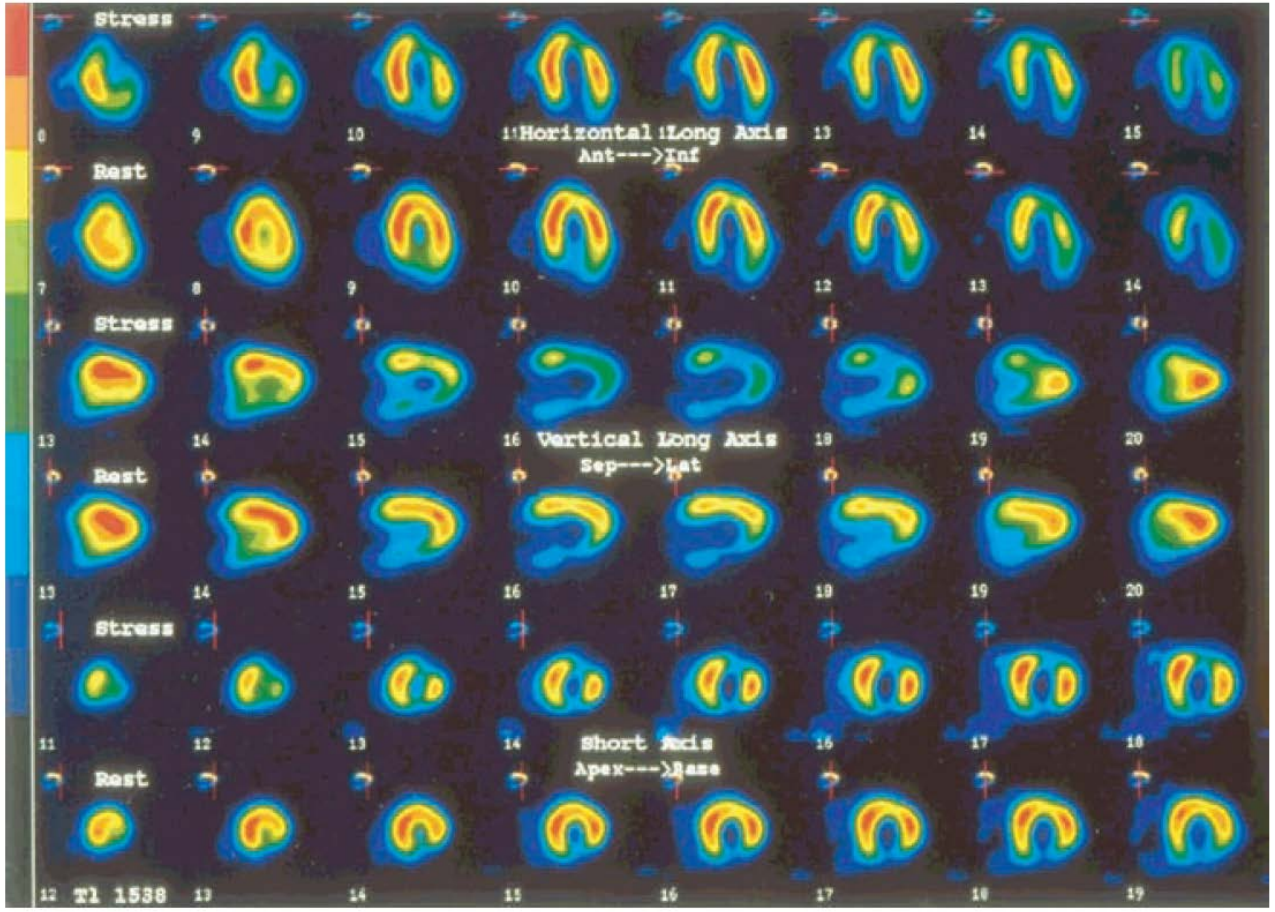

Fig. Myocardial perfusion SPECT scan. Rows 1, 3, and 5 show the myocardial perfusion during a typical stress test. Rows 2, 4, and 6 show the rest images acquired 3 hours later. The first two rows are horizontal long-axis slices, the middle two rows are vertical long-axis slices, and the bottom two rows are short-axis slices. This study shows a typical example of transient hypoperfusion of the anterior wall. On the stress images, there is a clear perfusion defect on the anterior wall (horizontal-axis slice 9, vertical long-axis 16 to 18, short-axis slice 13 to 18). The perfusion normalizes on the corresponding rest images.

Lung embolism

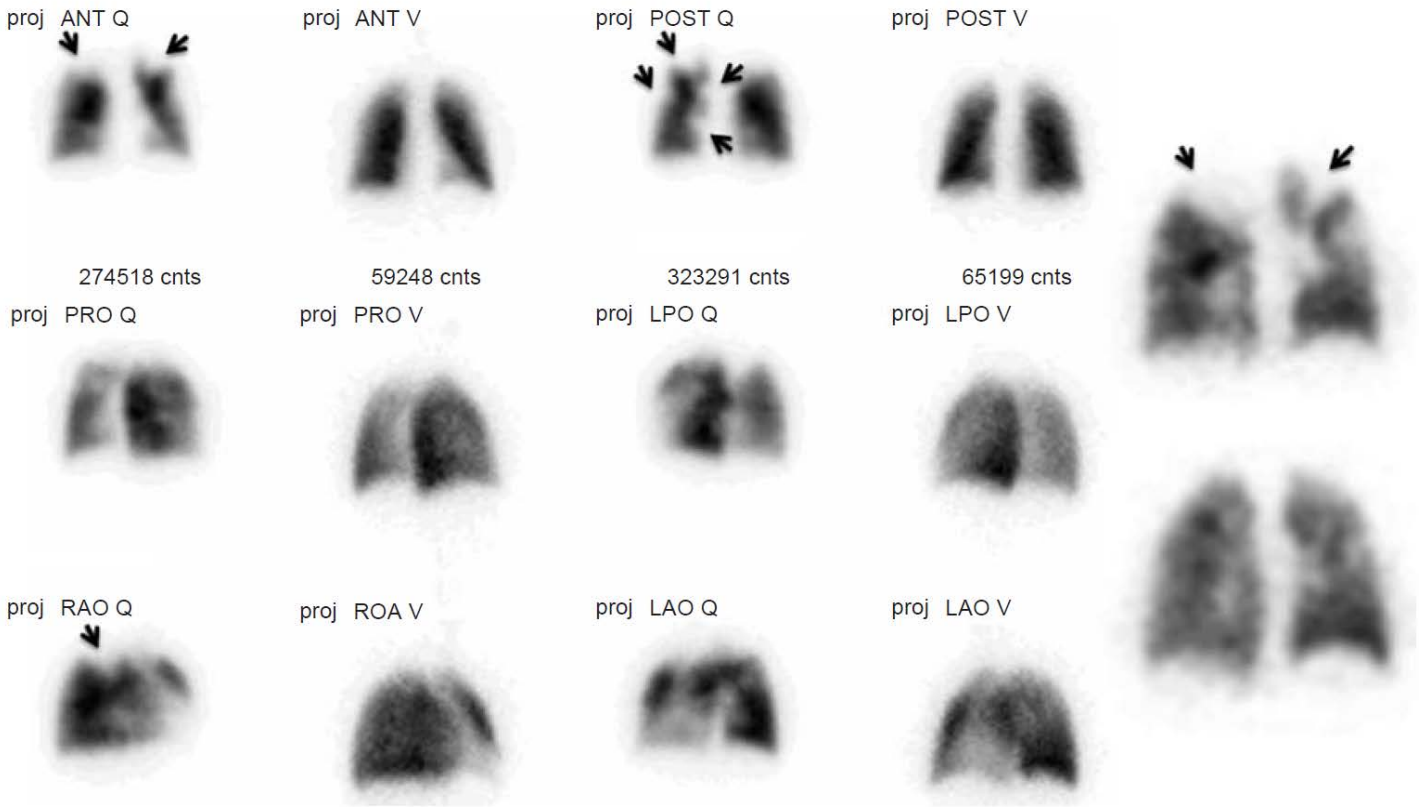

Fig. Lung perfusion (Q) and ventilation (V) scan. The second and fourth columns show six planar projections of a ventilation SPECT scan obtained after the inhalation of radioactive pertechnegas distributed homogeneously throughout both lungs. The first and third columns show the corresponding lung perfusion images obtained after injection of ^{99m}Tc-labeled macroaggregates. Several triangular-shaped defects (arrows) are visible in the perfusion scan with a normal ventilation at the same site. This mismatch between perfusion and ventilation is typical for lung embolism. The fifth column shows a coronal section of the SPECT data set with triangular defects (arrowheads) in the perfusion (upper row) and a normal ventilation (lower row).

Thyroid function

Fig. ^{99m}Tc pertechnetate thyroid scan of a patient with a multinodular goiter. The irregularly enlarged thyroid is delineated. Several zones of normal and increased uptake are visible. Hyperactive zones are seen in the upper and lower pole of the right thyroid lobe. In the right interpolar region there is a zone of relative hypoactivity.